Iranian Journal of Medical Physics

ijmp.mums.ac.ir

Optimization of Energy Window and Collimator for Y-90 Bremsstrahlung SPECT imaging: A Monte Carlo Simulation Study

Hicham Asmi[1], Farida Bentayeb[1], Youssef Bouzekraoui[1], Faustino Bonutti[2], Sanae Douama[1]

1. Department of Physics, LPHE, Modeling and Simulations, Faculty of Science, Mohammed V University, Rabat, Morocco
2. Academic Hospital of Udine, Department of Medical Physics, Udine, Italy

ARTICLE INFO

Article type:
Original Paper

Article history:
Received: Nov 30, 2019
Accepted: Apr 05, 2020

Keywords:
Y-90
SPECT imaging
Monte Carlo

ABSTRACT

Introduction: In yttrium-90 imaging, image quality is highly dependent on the selection of energy window and collimator design becausetheY-90 bremsstrahlung photons have a continuous and broad energy distribution. The current study aimed to optimize the bremsstrahlung energy window setting and collimator for the improvement of both resolution and sensitivity.
Material and Methods: In the present study, simulation of medical imaging nuclear detectors (SIMIND) Monte Carlo program was used to simulate Siemens Medical System Symbia. The SIMIND was utilized to generate the Y-90 bremsstrahlung single-photon emission computed tomography (SPECT) projection of the point source. Six energy windows settings and two collimators denoting medium energy and high energy were used in order to assess the effect of the energy window on the resolution.
Results: The experimental measurements and simulation results showed a similar pattern in the point spread functions with the energy window. The simulation data indicated that the geometric component reached 73%for the energy window within the range of51-120keVusingthe high-energy (HE) collimator. In addition, the obtained results showed that the full width at half maximum (FWHM) and full width at tenth maximum (FWTM)(FWHM=7mm and FWTM=35mm)were higher in this window in comparison to those reported for other windows.
Conclusion: According to the obtained results of the present study, the optimal energy window for Y-90 bremsstrahlung SPECT imaging was within the range of 51-120 keV. The obtained optimal energy window and optimal HE collimator had the potential to improve the image resolution and sensitivity of Y-90 SPECT images.

► *Please cite this article as:*
Asmi H, Bentayeb F, Bouzekraoui Y, Bonutti F, Douama S. Optimization of Energy Window and Collimator for Y-90 Bremsstrahlung SPECT imaging: A Monte Carlo Simulation Study. Iran J Med Phys 2021; 18: 263-269. 10.22038/ijmp.2020.44763.1691.

Introduction

The short half-life (T½=64.1 h) of the yttrium-90and its quasi-pure emission of high-energy (HE)beta particle smake it the privileged isotope in targeted radionuclide therapy for the treatment of non-Hodgkin's lymphoma and unresectable liver cancer [1-2].However,the Y-90 bremsstrahlung photons have a continuous and broad energy spectrum with high energy (Emax=2MeV). Therefore, the image quality is influenced by the photons detected in the energy window. Subsequently, the choice of collimator and energy window has a great effectonY-90 imaging.

Previous studies have used the Monte Carlo simulation to select theappropriate collimator and energy window settings for the bremsstrahlung single-photon emission computed tomography (SPECT) of Y-90 [3-10].The photons are classified according to their history in the collimator, including the geometric photons (passing through a collimator hole), scatter photons (scattering in the collimator or object), and penetration photons (penetrating the collimator and not scattering in the collimator or object).Moreover, the photons absorbed in the collimator septa can provide X-ray components[11].Only the geometric photons provide correct positional information.

The simulation of medical imaging nuclear detectors (SIMIND) Monte Carlo code uses the delta scattering methods to sample the interaction of photons through the collimators. Therefore, SIMIND Monte Carlo program can accurately simulate all the interaction of photons inside the collimator. Subsequently, the accurate assessment of the geometric, penetration, and scattered contributions inside the photo peak window can be carried out using the Monte Carlo simulation technique.

**Corresponding Author:* Tel: +212623609312; Email: youssef0fsr@gmail.com

Several studies were conducted on SIMIND Monte Carlo simulation program to determine the different components of detected radiation [3,10].

Bremsstrahlung imaging makes it difficult to choose collimator and energy window; therefore, the optimal clarity of the image is not always achievable. With this background in mind, the present study used the SIMIND Monte Carlo code for the estimation of the geometric, penetration, and scatter components for parallel-hole collimators. The Y-90sensitivityis very low because approximately 1% of the kinetic energy of the β-particle is emitted in the form of Bremsstrahlung radiation decreasing the image quality. To overcome this problem, (i.e., increasing the sensitivity), a large window could be used; however, it includes a large contribution of scattered photons. In this study, six narrow energy windows and two collimators were utilized in order to optimize the tradeoff between the sensitivity and resolution for Y-90 bremsstrahlung imaging.

Materials and Methods

In the present study, the SIMIND program(6.2)[12]was used to simulate Siemens Medical System Symbia equipped with a detector with NaI(Tl) crystal thickness of 0.95 cm, intrinsic spatial resolution of 0.45 cm, and energy resolutionof8.80% at 140 keV. The dimension of the crystal was 59.1 × 44.5 cm^2. A 0.05-cm diameter point source filled with Y-90 (3.7MBq) was placed at 15 cm from the detector and located in a cylindrical water phantom (with a diameter of 16 cm and length of 32 cm).The acceptance angle of photons emitted toward the camera was set at45.The pixel size in the simulated planar source images is 0.34 cm and 128 × 128 matrix size.

At the end of the simulation, the SIMIND code produces a planar image with float values (real *4). Then, these images were imported to ImageJ software [13]. This simulation included two collimators, including medium-energy (ME) and HE collimators (Table 1). Six energy windows were chosen within the range of10-580keV (Table 2). Figure 1 illustrates the SIMIND simulation of Y-90 for point source.

The SIMIND program has two main programs, namely CHANGE defining the system parameters and SIMIND executing the simulation. Moreover, the desired parameters of the system can be introduced using CHANGE program. At the end of simulation, SIMIND program provided the values of geometric, penetration, scatter, and X-ray components and images in separate files. The simulated Y-90 images were quantitatively evaluated using spatial resolution (i.e., the full width at half maximum [FWHM] and full width at tenth maximum [FWTM]) for both the HE and ME collimators.

Table 1.Data of collimators

Diameter(cm)	Septa(cm)	Length(cm)	Hole shape	Collimator type	Collimator
0.294	0.114	4.064	Hexagonal	Parallelhole	Medium-energy
0.400	0.200	5.970	Hexagonal	Parallelhole	High-energy

Table 2.Used energy windows during simulation

Windows (keV)	(10.50)	(51.120)	(121.189)	(190.259)	(260.329)	(330.580)
Center (keV)	30	85	154	224	294	485

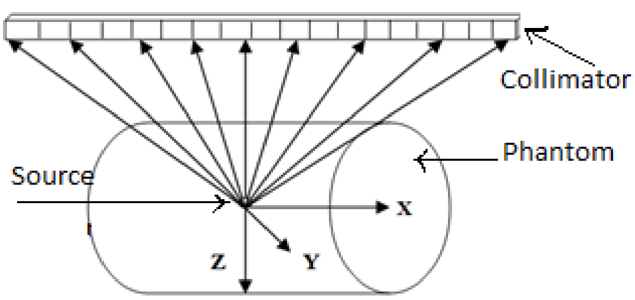

Figure 1.Geometry of simulation

Results

In this study, the geometric, septal penetration, scattering, and X-ray components in parallel-hole collimators (i.e., ME and HE) were assessed by a Y-90point source with six energy windows within the range of 10-580 keV (Figure 2) using the SIMIND Monte Carlo code. Table 3 tabulates the results of the simulation. Figure 3 depicts the variation of geometric, penetration, scatter, and X-ray components with the energy window in ME and HE collimators, respectively.

The geometric component decreases with the energy window; nevertheless, the penetration and scatter components increased with raising the energy window. It was noted that the geometric component reached 83% and 63% for the HE and ME collimators in the energy window of 51-120keV, respectively. The high penetration and scatter components were due to the large spectrum of Y-90 (up to 2000keV).According to Figure 3, it is clear that the penetration and scatter are significant problems for ME making this collimator less useful for imaging. Moreover, even for the HE collimator, the penetration and scatter effects were also significant. Figures 3 and 4 illustrate the images of the Y-90point source obtained through the experiment and simulation, respectively.

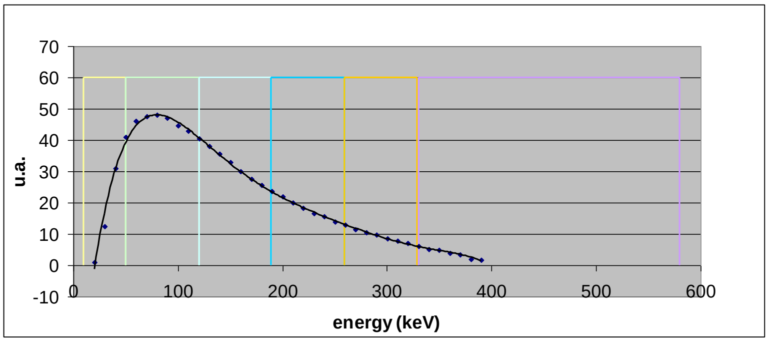

Figure 2.Energy spectra of yttrium-90 bremsstrahlung photons from point source

Table 3.Results of simulation

Collimator	Energy window	Geometric (%)	Penetration (%)	Scatter (%)	X-ray
Medium-energy	(10-50)	63.55	16.28	19	1.1
	(51-120)	56.89	17.98	18.59	6.54
	(121-189)	32.87	31.77	35.37	0
	(191-259)	13.64	48.32	38.04	0
	(260-329)	7.33	44.97	47.7	0
	(330-580)	2.39	46.47	51.14	0
High-energy	(10-50)	83.3	5.78	10.22	0.7
	(51-120)	72.62	8.6	13.4	5.38
	(121-189)	61.17	16.31	22.52	0
	(191-259)	32.49	26.12	41.38	0
	(260-329)	17.44	32.19	50.37	0
	(330-580)	6.03	31.01	62.96	0

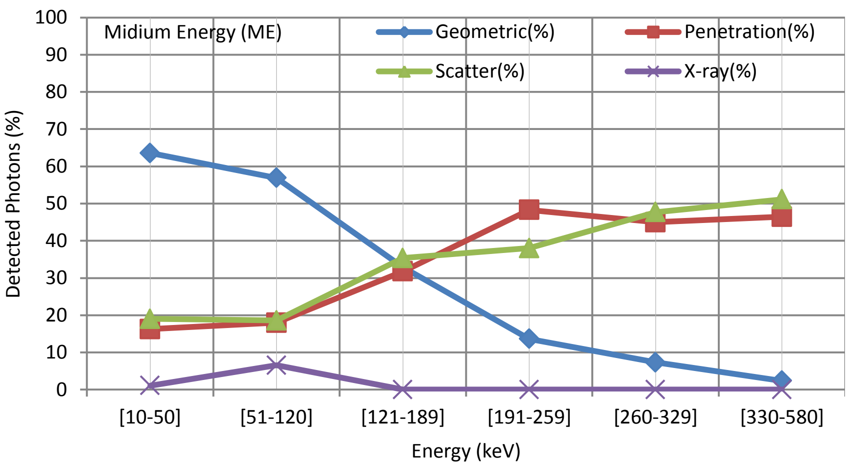

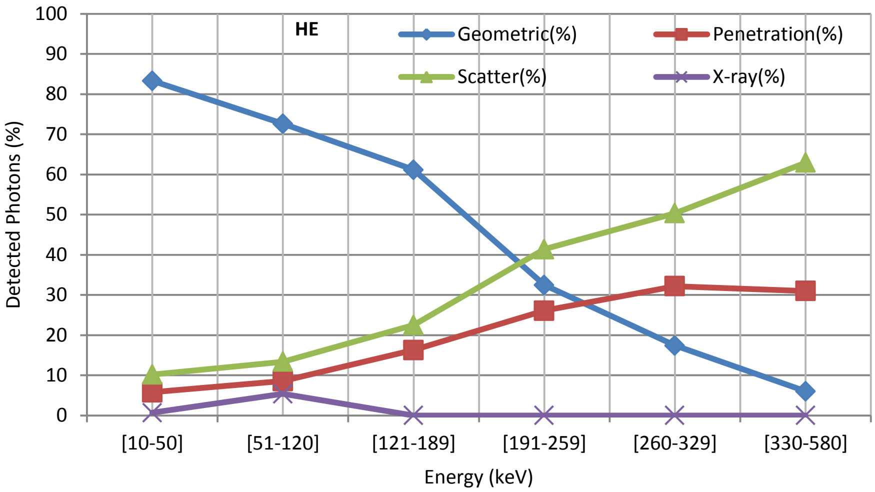

Figure 3.Variation of geometric(i.e., detected photons on detectorwithout any scatter or penetration), penetration(i.e., photons passedthrough septa without attenuation), scatter (i.e., photonsscattering in collimator)and X-ray(i.e., photons absorbed in septacollimator) componentsas a function of center energy formedium-energyand high-energycollimators

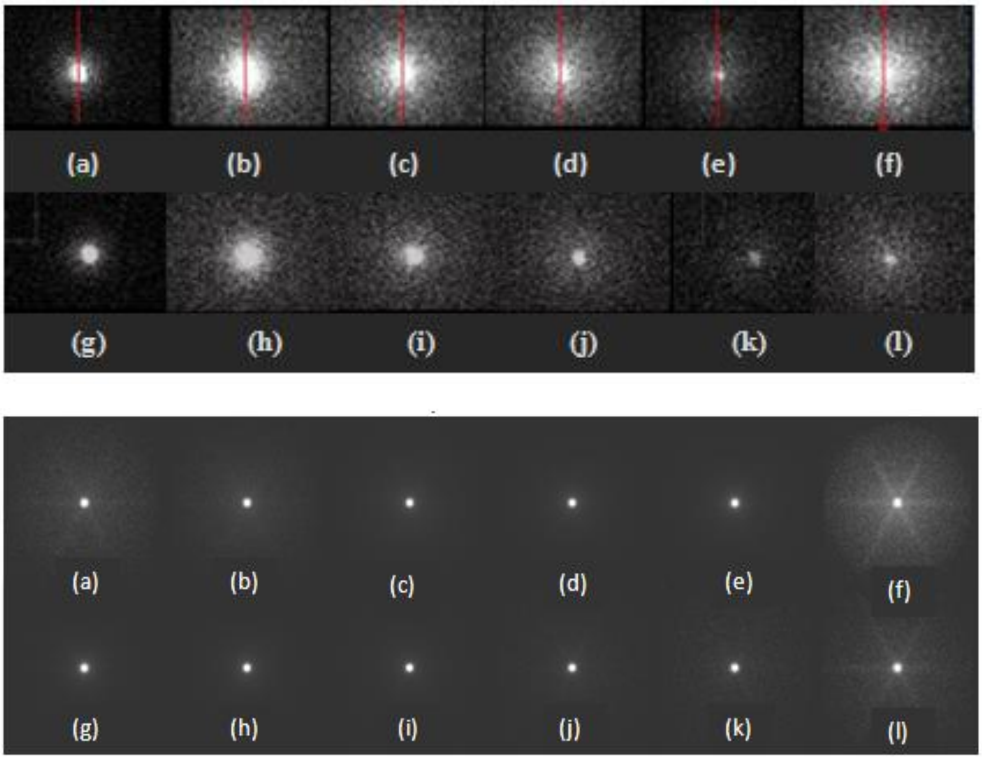

Figure 4.Image of yttrium-90 point source obtained through experiment (above images) and simulation (below images) in energy window widths of(a,g) 10-50, (b,h) 51-120, (c,i) 121-189, (d,j) 190-259, (e,k) 260-329, and (f,l) 330-580keV for medium-energy and high-energy collimators

Table 4.Full width at half maximumobtained from point source images of Figure 4

Collimator	Energy window	FWHM(mm)	FWTM(mm)	cps/MBq
Medium-energy	(10-50)	7.05	36.45	1.27
	(51-120)	6	49.03	1.82
	(121-189)	5.94	36.92	3
	(191-259)	8.26	47.87	1.34
	([260-329)	2.19	39.13	0.84
	(330-580)	3.36	72.96	2.25
High-energy	(10-50)	7.42	30.06	0.71
	(51-120)	6.59	35.12	1.63
	(121-189)	6.23	28.75	0.78
	(191-259)	4.39	29.63	0.4
	(260-329)	3.6	20.09	0.21
	(330-580)	5.56	35.26	0.9

FWHM:Full width at half maximum
FWTM: Full width at tenth maximum

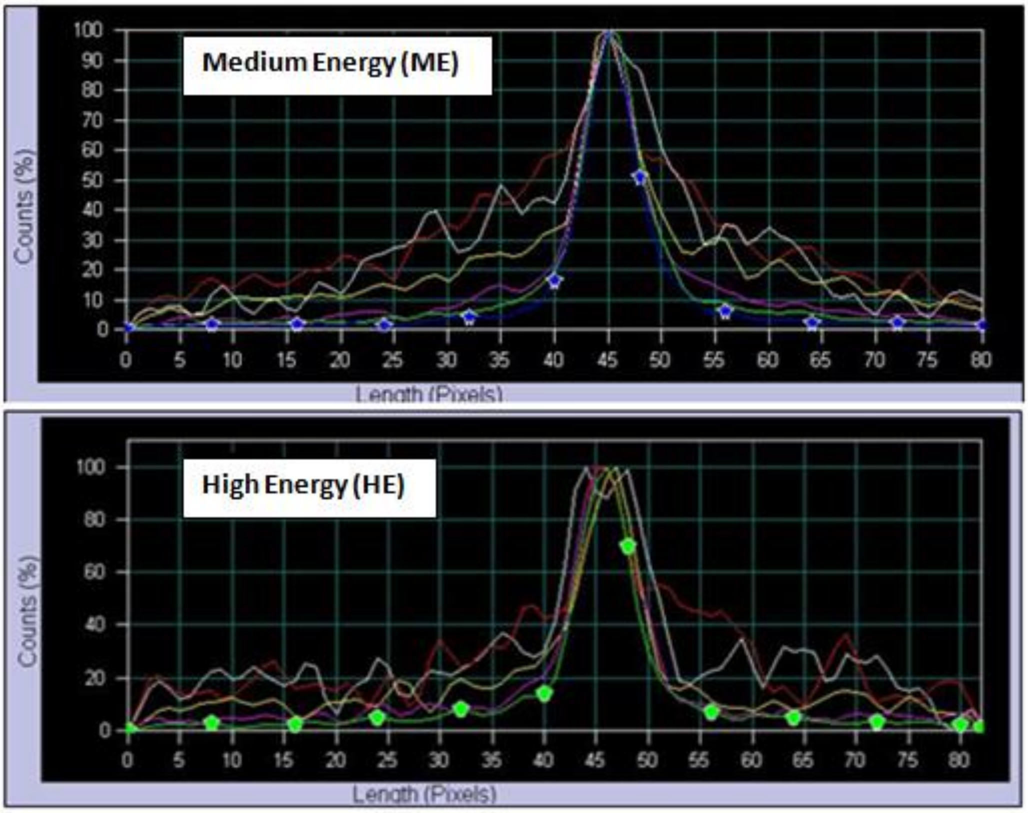

Figure 5. Experimental point spread functions and number of pixels: 30 keV-blue, 85keV-green, 154keV-magenta, 224keV-yellow, 294keV-white, and 485keV-red

The absence of pronounced photo-peak energy of bremsstrahlung photons was the main reason for the poor quality of the Y-90 point source image (by the simulation and experiment) obtained by HE and ME collimators for .This is evident from the calculated values of high septa penetration and scattering obtained as a result of the simulation in Table 3. It is important to mention that the foggiest images had the highest values of penetration and scatter for both collimators.

The 6-fold symmetry of tails was associated with the hexagonal-hole shape of the collimator used in the simulation. The measured and simulated spatial distribution of the point spread functions (PSFs) of the photons detected in the six-energy window is depicted in Figure 4 and 5 respectively. To characterize the point source profiles, the FWHM was not sufficient due to the presence of the tails at the sides of the PSFs; therefore, the FWTM should also be assessed in this regard. The

FWHM and the FWTM were computed on the simulated PSFs. Table 4 tabulates the results of both FWHM and FWTM.

Table 4 illustrates the values of the FWHM and FWTM **7**for the PSFs normalized at their maximum values. According to Figure 5, the ME collimator increases the FWTM. For all energy windows, there was a higher FWTM (less spatial resolution) for the ME collimator in comparison to that reported for the HE collimator. The calculated sensitivities in six energy windows are listed in Table 4.

The FWHM and FWTM were higher (FWHM=7mm and FWTM=35.06mm) in the 51-120 keV window than another window for the HE collimator. The HE sensitivity was lower than the ME sensitivity for six energy windows as shown in Figure 8.The spatial resolutions (FWHM=7mm and FWTM=35.06mmat 51-120 keV) observed with the collimator were the best spatial resolutions with the consideration of noticed HE sensitivity. The ME collimator had higher sensitivity and septal penetration; however, the HE collimator gave a lower sensitivity and septal penetration.

Discussion

Scattered and penetration photons through the collimator septal are the degrading effects of images in the Y-90 bremsstrahlung SPECT imaging. Fora particular selection of collimators, the fogginess of the images changes with the energy window. Good image quality can be achieved in case of using the HE collimator. Based on the profiles, the FWHM and FWTM were determined and observed as significantly varied with energy windows for both collimators.

The HE collimator offers higher resolution than the ME collimator for all energy windows. The Y-90 sensitivity is related to image noise, which can be important for detecting small amounts of activity. The sensitivity (cps/MBq) was calculated as the ratio of the total counts in the field of vision and acquisition activity. The collimators have an inverse relationship with parallel holes, sensitivity, and spatial resolution. A longer hole means higher spatial resolution but low sensitivity. Therefore, a range of collimators is often used to achieve the optimal compromise between sensitivity and resolution.

To improve sensitivity, a large energy window was used; nevertheless, this can lead to a decrease in resolution. The ME collimator offered higher sensitivity and lower spatial resolution, compared to the HE collimator, because the HE collimator reduced septal penetration with thicker septa. Therefore, the determination of collimator and energy window for Y-90 imaging is a compromise between sensitivity and spatial resolution.

Conclusion

The present study evaluated the effect of the parallel-hole collimators and energy window on the resolution and sensitivity of Y-90 point source using the SIMIND Monte Carlo program. The obtained results of the current study indicated that the best compromise between the sensitivity and resolution was reached in case of using an energy window of 51-120 keV.

Acknowledgment

The authors are grateful to the International Atomic Energy Agency (IAEA) for their sincere cooperation.

References

1. Stigbrand T, Carlsson J, Adams GP, editors. Targeted radionuclide tumor therapy: Biological aspects. New York: Springer; 2008 Sep 1.
2. Nag S, Kennedy A, Salem R, Murthy R, McEwan A, Nutting C, et al. Recommendations for radioembolization of hepatic malignancies using Yttrium-90 microsphere brachytherapy: A consensus panel report from the Radioembolization Brachytherapy Oncology Consortium (REBOC). Brachytherapy. 2007 Apr 1;6(2):116-7.
3. Rong X, Frey EC. A collimator optimization method for quantitative imaging: Application to Y-90 bremsstrahlung SPECT. Medical physics. 2013 Aug;40(8):082504.
4. Rong X, Ghaly M, Frey EC. Optimization of energy window for 90Y bremsstrahlung SPECT imaging for detection tasks using the ideal observer with model-mismatch. Medical physics. 2013 Jun;40(6Part1):062502.
5. Rong X, Du Y, Frey EC. A method for energy window optimization for quantitative tasks that includes the effects of model-mismatch on bias: application to Y-90 bremsstrahlung SPECT imaging. Physics in Medicine & Biology. 2012 May 23;57(12):3711.
6. Heard S, Flux GD, Guy MJ, Ott RJ. Photon source kernels for Monte Carlo simulation of bremsstrahlung imaging. Ineuropean journal of nuclear medicine and molecular imaging. 2004 Aug 1; 31:403.
7. Shen S, Denardo G, Yuan A, Denardo D and Denardo S. Planar gamma-camera imaging and quantitation of Y-90 bremsstrahlung. J. Nucl. Med. 1994;35:1381‑9.
8. Yue J, Mauxion T, Reyes DK, Lodge MA, Hobbs RF, et al. Comparison of quantitative Y-90 SPECT and non-time-of-flight PET imaging in post-therapy radio embolization of liver cancer. Med Phys. 2016 Oct;43(10):5779.
9. Elschot M, Vermolen B, Lam M, de Keizer B, van den Bosch M, de Jong H. Quantitative comparison of PET and SPECT for imaging the yttrium-90 microsphere distribution after liver radio embolization. Journal of Nuclear Medicine. 2012 May 1;53(supplement 1):103.
10. Bouzekraoui Y, Bentayeb F, Asmi H, Bonutti F. Energy window and contrast optimization for single-photon emission computed tomography bremsstrahlung imaging with yttrium-90. Indian journal of nuclear medicine: IJNM: the official journal of the Society of Nuclear Medicine, India. 2019 Apr;34(2):125.
11. De Vries DJ, Moore SC. Approximation of hexagonal holes by square holes in Monte Carlo

simulation of gamma-camera collimation. IEEE Transactions on Nuclear Science. 2002 Dec 10;49(5):2186-95.

12. Ljungberg M. The SIMIND Monte Carlo program home page. 2018. Available from: https://www.msf.lu.se/research/the-simind-monte-carlo-program.
13. Ferreira T.Rasband W. Image J Program. 2018. Availablefrom:https://imagej.nih.gov/ij/download.html.